THE SOMATIC SHUNT CABLE MODEL FOR NEURONS

DOMINIQUE DURAND
Addiction Research Foundation, Institute of Biomedical Engineering, University of Toronto, Playfair Neuroscience Unit, Toronto Western Hospital, Toronto, Canada, and Applied Neural Control Laboratory, Department of Biomedical Engineering, Case Western Reserve University, Cleveland, Ohio 44106

ABSTRACT The derivation of the equations for an electrical model of nerve cells is presented. The model consists of an equivalent cylinder, a lumped somatic impedance, and a variable shunt at the soma. This shunt was introduced to take into account the fast voltage decays observed following the injections of current pulses in some motoneurons and hippocampal granule cells that could not be explained by existing models. The shunt can be interpreted either by penetration damage with the electrode or by a lower membrane specific resistance at the soma than in the dendrites. A solution of the model equations is presented that allows the estimation of the electrotonic length L, the membrane time constant τ_m, the dendritic dominance ratio ρ, and the shunt parameter ϵ, based only on the measurement of the first two coefficients and time constants in the multiexponential voltage response to injected current pulses.

INTRODUCTION

The Rall cable model of neurons has been widely used to determine the electrical properties of nerve cells. In this model, the dendritic tree is replaced by an equivalent cylinder and the soma by a lumped impedance. The assumptions underlying the derivation of the equations have been reviewed by Rall (1977). Although these equations have been shown to account for the voltage decays from current pulses injected through intracellular electrodes, some evidence suggests that this model does not accurately explain the fast potential decays observed in some neurons. Iansek and Redman (1973) and Durand et al. (1983) reported that only 30% of motoneurons and 40% of hippocampal granule cells could accurately be fitted by this cable model. The faster than expected experimental transients suggested the presence of a shunt located at the soma, perhaps caused by electrode penetration damage or a decreased somatic resistance. The effect of a low resistance at the soma is to decrease the somatic time constant and accelerate the potential decay as observed experimentally. The presence of electrode damage at the soma caused by penetration has been suspected for a long time, but there is no easy way to measure it. Similarly, a somatic membrane resistance lower than the dendritic membrane resistance could also be responsible for a somatic shunt, both in motoneurons and in granule cells where many inhibitory inputs synapse at the soma. Recently (Fleshman et al., 1983), a linearly increasing membrane resistance model (low membrane resistance at the soma) for motoneurons was introduced to provide a better fit of the experimental data. It is not possible, however, to distinguish between a shunt caused by penetration damage and a decreased somatic resistance. Therefore, a new parameter, ϵ, is introduced to account for a lower somatic time constant, τ_s, compared with the membrane time constant τ_m, and it is defined by $\epsilon = \tau_s/\tau_m$ (Durand and Kunov, 1982). The solution of the cable partial differential equation with new boundary conditions is outlined below, and the equations for either a shunt caused by electrode penetration or by a decreased somatic resistance are derived. The inverse problem of finding the model parameters, given the time constants and coefficients of the voltage decay, is also solved.

GLOSSARY

R_m	membrane specific resistance ($\Omega \cdot cm^2$)
C_m	membrane specific capacitance ($\mu F/cm^2$)
R_i	axoplasmic specific resistance ($\Omega \cdot cm$)
τ_m	membrane time constant = $R_m C_m$ (s)
D	diameter of the equivalent cable (cm)
λ	space constant = $(R_m \cdot D/4 \cdot R_i)^{1/2}$ (cm)
ℓ	length of the equivalent cable (cm)
L	electrotonic length = $1/\lambda$
R_s	resistance of the soma (Ω)
R_D	input resistance of the dendritic equivalent cable (Ω)
R_N	input resistance of the cell (Ω)
ρ	dendritic dominance ratio = R_s/R_d
V	potential across the membrane (the resting potential is assumed to be equal to zero) (V)
x	distance along the cable (cm)
t	time (s)
τ_0, τ_1, τ_2	equalizing time constants
C_0, C_1, C_2	coefficients of the several exponential in the voltage decay (V)
α_i	eigenvalues of the boundary problems
α	separation constant

Address reprint requests and correspondence to Dr. Dominique Durand, Applied Neural Control Laboratory, Department of Biomedical Engineering, Case Western Reserve University, Cleveland, Ohio 44106.

B_i coefficients of infinite series solutions
τ_s time constant of the somatic membrane (s)
I current injected at the soma (A)
ϵ somatic shunt parameter = τ_s/τ_m.

RESULTS

The model consists of a single cable of electrotonic length L with two known boundary conditions (see Fig. 1). The equation describing the electrical behavior of such a system is known as the cable equation (Rall, 1959, 1969, 1977):

$$\frac{\partial^2 V}{\partial X^2} - V - \frac{\partial V}{\partial T} = 0. \tag{1}$$

V is the potential along the cable and is a function of distance X and time T. X and T are the normalized space and time variables defined by:

$$X = x/\lambda; \tag{2}$$

$$T = t/\tau_m, \tag{3}$$

where λ and τ_m are the space and membrane time constants, respectively.

The mathematical treatment of core conductors has been applied to neurons by many researchers (Hodgkin and Rushton, 1946; Davis and Lorente de No, 1947; Rall, 1959, 1969, 1977). A detailed review of the assumptions and derivation of the cable equation was published by Rall in 1977. The steady state and transient solutions for the equation with the new boundary conditions will be derived below.

At the sealed end or open termination ($X = L$), the voltage follows the following equation, since no current can leave the cable (Rall, 1969):

$$\left(\frac{\partial V}{\partial X}\right)_{X=L} = 0. \tag{4}$$

At the somatic end ($X = 0$), when the input current has been turned off, we have:

$$I_S = -I_D. \tag{5}$$

I_S is the current flowing in the soma and I_D is the current flowing into the dendritic tree. The current I_S can be expressed by the sum of the current in the resistance (I_R)

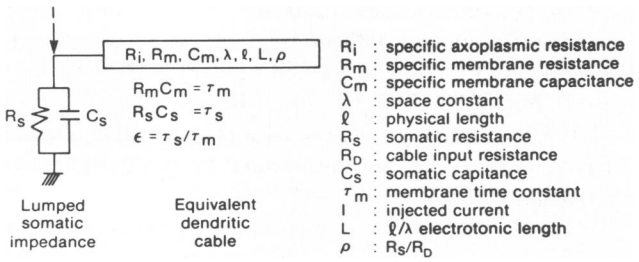

FIGURE 1 The shunt model: a somatic shunt due to either electrode or injury or decreased somatic resistance is introduced with parameter $\epsilon = \tau_s/\tau_m$. ϵ is always ≤ 1 and $\epsilon = 1$ corresponds to the case of the Rall model.

and in the capacitance (I_C) (see Fig. 1):

$$I_S = I_R + I_C = \frac{V}{R_s} + C_s \cdot \frac{\partial V}{\partial t} \tag{6}$$

$$= \frac{1}{R_s} \cdot V + \frac{\tau_s}{\tau_m} \cdot \frac{\partial V}{\partial T} = \frac{1}{R_s} V + \epsilon \cdot \frac{\partial V}{\partial T}, \tag{7}$$

with $\epsilon = \tau_s/\tau_m$.

The current I_D can be calculated by applying Ohm's law for a core conductor. The longitudinal current, I_i, is given by the expression

$$I_i = -\frac{\partial V}{\partial x} \cdot \frac{1}{r_i}, \tag{8}$$

where r_i is the axoplasmic resistance per unit length.

Therefore, at $X = 0$, we have

$$I_D = -\frac{1}{\lambda r_i} \cdot \left(\frac{\partial V}{\partial X}\right)_{X=0}. \tag{9}$$

Combining Eqs. 6, 7, and 9, we obtain:

$$\left(\frac{\partial V}{\partial X}\right)_{X=0} = \frac{\lambda r_i}{R_s} \cdot \left(V + \epsilon \frac{\partial V}{\partial T}\right)_{X=0}$$

$$= \frac{\tanh L}{\rho} \cdot \left(V + \epsilon \frac{\partial V}{\partial T}\right)_{X=0}, \tag{10}$$

where ρ is defined as the dendritic to somatic conductance ratio (Rall, 1969), and is equal to $R_s/\lambda r_i \cdot \coth L$ (Rall, 1977). By the separation of variables method, it can be shown that a particular solution of the differential Eq. 1 is:

$$V(X,T) = [B_1 \cos\alpha(L - X) + B_2 \sin\alpha(L - X)]\, e^{-(1+\alpha^2)T}, \tag{11}$$

where α is the separation constant.

Applying the boundary conditions of Eqs. 4 and 10, we now obtain $B_2 = 0$ and the following transcendental equation:

$$L \cdot \cot \alpha L \cdot \frac{1 - \epsilon(1 + \alpha^2)}{\alpha} = \rho L \coth L = k, \tag{12}$$

where k is a constant. This equation has an infinite number of solutions α_n plotted in Fig. 2. The general solution to the cable equation for the voltage response following the injection of a step current pulse of amplitude I at $X = 0$ beginning at $T = 0$ is an infinite sum of exponentials obtained from Eq. 11, where $B_2 = 0$ (Rall, 1977):

$$V(X, T) = V(X, \infty) - \sum B_i \cos \alpha_i (L - X)\, e^{-(1+\alpha_i^2)T}. \tag{13}$$

The function $V(X, \infty)$ is the steady state voltage distribution in the cable following the injection of a current pulse at $X = 0$ and is given by Eq. 4.18 in Rall (1977) since the somatic boundary conditions in this problem do not effect $V(X, \infty)$.

At $T = 0$, $V(X, T) = 0$, and therefore we obtain the

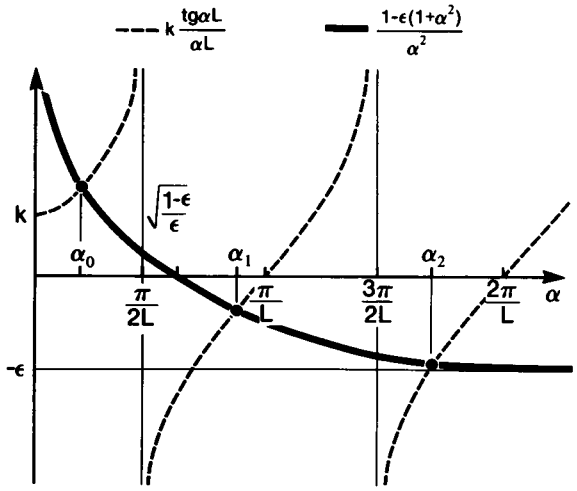

FIGURE 2 A graphical solution of the transcendental boundary equation is given, $[1 - \epsilon(1 + \alpha^2)]/\alpha^2 = k \tan(\alpha L)/(\alpha L)$. There is an infinite number of solutions α_n given by the intersection of the solid line (left side of the above equation) and the dashed line (right side). Because the function $[1 - \epsilon(1 + \alpha^2)]/\alpha^2$ is monotonous, only one such set of solutions satisfies the boundary equation and therefore the α_n gives a unique solution for the model.

following equation:

$$V(X, \infty) = IR_N \cdot \frac{\cosh(L - X)}{\cosh L} = \sum_i B_i \cos \alpha_i (L - X). \quad (14)$$

This is a generalized Fourier series and the coefficients B_i are called the Fourier coefficients with respect to the set of functions $X_i = \cos \alpha_i(L - X)$. These coefficients are easily determined if the set of functions X_i is orthogonal. However, it can be shown (Durand, 1982) that this set of functions is not orthogonal and therefore the usual method cannot be employed. An alternative solution is provided by the modified orthogonality relation of Churchill (1942):

$$B_n = \frac{B[V(X, \infty), X_n]}{B(X_n, X_m)}, \quad (15)$$

where

$$B(f, g) = \int_0^L f \cdot g dX + b_0 f(0)y(0) + b_1 f(L)g(L),$$

and b_0 and b_1 are defined by the boundary equations

$$a_0(X_n)_{x=0} + \left(\frac{dX_n}{dX}\right)_{x=0} + b_0\left(\frac{d^2X_n}{dX^2}\right)_{x=0} = 0;$$

$$a_1(X_n)_{x=0} + \left(\frac{dX_n}{dX}\right)_{x=0} + b_1\left(\frac{d^2X_n}{dX}\right)_{x=0} = 0.$$

Using the above method, the equation for the voltage decay $V(t)$ following a step current pulse injected at $X = 0$ is derived in Appendix I and is given as:

$$V(t) = IR_N - \sum_i C_i e^{-t/\tau_i}, \quad (16)$$

where τ_i = equalizing time constants obtained from Eq. 13:

$$\tau_i/\tau_m = 1 + \alpha_i^2 \quad (17)$$

and α_i are solutions of the following transcendental equation derived from Eq. 12:

$$\alpha_i L \beta_i \cot \alpha_i L - \rho L \coth L \quad (18)$$

$$\beta_i = [1 - \epsilon(1 + \alpha_i^2)]/\alpha_i^2 \quad (19)$$

and

$$C_i = IR_N \cdot \frac{2(\rho + 1)\tau_i/\tau_m}{\beta_i + 2\epsilon + k + (\alpha_i\beta_i L)^2/k} \quad (20)$$

with

$$k = \rho L \coth L. \quad (21)$$

The particular case of $\epsilon = 1$: If ϵ is set to 1 in Eqs. 18, 19, and 20, these equations should reduce to the case of a model with a uniform time constant derived by Rall (1977). If $\epsilon = 1$, then $\beta_i = -1$, and C_i is equal to (Eqs. 4.21 and 4.22 in Rall [1977]):

$$C_i = IR_N \cdot \frac{(\rho + 1)}{(k + 1)} \cdot \frac{2\tau_i/\tau_m}{1 + (\alpha_i L)^2/(k^2 + k)}.$$

Voltage Response to a Short Current Pulse

The voltage decay following a short current pulse of width W injected at $X = 0$ is given by:

$$V_s(t) = C_{si} e^{-t/\tau_i} \quad (22)$$

with the coefficients C_{si} obtained from the long pulse coefficients C_i by the equations derived in Durand et al. (1983):

$$C_{si} = C_i (1 - e^{-W/\tau_i}). \quad (23)$$

Therefore,

$$C_{si} = IR_N \cdot \frac{(1 - e^{-w/\tau_i}) \cdot 2(\rho + 1) \cdot \tau_i/\tau_m}{\beta_i + 2\epsilon + k + (\alpha_i\beta_i L)^2/k}. \quad (24)$$

Numerical Example

To illustrate the effects of the somatic shunt, the time constant and coefficients resulting from a short pulse current injection into a theoretical cell were calculated. The parameters chosen for the cell were: $\tau_m = 10$ ms; $L = 1$; $\rho_{NS} = 5$; $R_{NS} = 100$ MΩ; $I = 2$ nA, $W = 0.5$ ms; $G = 100$; $\epsilon = 1, 0.9, 0.8, 0.5, 0.1, 0.05$. Eq. 24 was modified to include the gain G of the recording system by multiplying the coefficient IR_N by G.

The subscript NS refers to parameters with no shunt ($\epsilon = 1$). The solutions α_0 and α_1 Eq. 19 were first determined by an iteration procedure in which a starting value α_0 was increased until a solution was found. The time constants and coefficients were then evaluated with Eqs.

17, 19, and 20. The results corresponding to a cell with the parameters mentioned above are tabulated in Table I. Note that the equalizing time constant τ_0, which corresponds to the uniform exponential decay of the voltage along the dendritic tree, always remains between τ_s and τ_m and drops as expected with increasing shunt amplitudes (decreasing values of ϵ). The effect of decreasing values of ϵ is also to lower the input resistance R_N and the coefficient of the first exponential C_0, although C_1 and τ_1 are much less affected. A 76% decrease in input resistance causes only a 33% decrease in τ_1 and a 19% decrease in C_1. ρ is also drastically decreased and, as suggested by Rall (1977), a shunt at the soma could explain the variability in the measurement of ρ reported in the literature. Assuming that the shunt is caused by penetration damage, the resting potential, E, is calculated to determine how it is affected by decreasing the value of ϵ.

Alternative Interpretations of the Somatic Shunt

As mentioned above, a lower somatic time constant can have several interpretations. Two of these interpretations are explored and illustrated by numerical examples below.

Electrode Penetration Damage. If a resistor R_{SH} (SH stands for shunt) is placed in parallel with the somatic resistor R_s (see Fig. 3), then the somatic time constant $\tau_s = [(R_{SH} \cdot R_s/(R_{SH} + R_s)] \cdot C_S$ will be lower than the time constant $\tau_m = R_sC_s = R_mC_m$. This type of shunt corresponds to a possible electrode injury at the impalement site. In this case, it is easy to show (Durand, 1982) that the input resistance of the cell (R_{NS}) and the resting potential (E_{NS}) before impalement can be obtained from the measured values of R_N and E multiplied by $(\rho + 1)/(\rho + \epsilon)$. The effects of the somatic shunt parameter, ϵ, on the measured resting potential, E, are tabulated in Table I. Also, in this case, the membrane somatic specific resistance R_{ms} is equal to the dendritic specific resistance R_{md} and can be calculated by:

$$R_{ms} = R_{md} = R_m = R_s \cdot S = R_N \cdot S \cdot (\rho + 1)/\epsilon, \quad (25)$$

where S is the somatic surface area.

Decreased Somatic Specific Resistance. A decrease in the somatic time constant can also be interpreted by a low value of the membrane specific resistance R_{ms} compared with the membrane specific resistance of the dendrites R_{md}. (It is assumed that the specific membrane capacitance C_s is the same for both the soma and the dendrites.) In this case, it can easily be shown (Durand, 1982) that:

$$R_{ms} = R_S \cdot S = R_N \cdot (\rho + 1) \cdot S \quad (26)$$

and

$$R_{md} = R_{ms}/\epsilon. \quad (27)$$

Numerical Example. If we choose a neuron with the parameters $R_N = 85.71$ MΩ, $\rho = 2.5$, $\epsilon = 0.5$, $E = 60$ mV, $S = 500$ μm², $\tau_m = 10$ ms, it can be calculated that in the case of electrode penetration shunt: $R_{NS} = 100.00$ MΩ, $E_{NS} = 70$ mV, $R_{ms} = 3{,}000$ Ω · cm², $C_m = 3.3$ μF/cm².

In the case of decreased somatic specific resistance from Eqs. 30 and 31, the following parameters can be calculated: $R_N = 85.7$ MΩ, $E = 60$ mV, $R_{ms} = 1{,}500$ Ω · cm², $C_m = 3.3$ μF/cm², and $R_{md} = 3{,}000$ Ω · cm². The coefficients and time constants of the voltage decay following the injection of the same current pulse would be identical in both cases. However, this example shows how different the interpretations of the results can be on the measurement of the specific parameters. A neuron impaled with an electrode causing injury to the membrane and a drop in the resting potential of only 10 mV is electrically equivalent to a neuron with a somatic specific resistance two times smaller than the dendritic specific resistance. The two neurons would have the same measured input resistance and time constants as calculated above.

TABLE I

THEORETICAL CALCULATIONS OF COEFFICIENTS AND TIME CONSTANTS IN A CELL WITH ELECTROTONIC LENGTH OF $L = 1$, AND AFTER INJECTION OF A CURRENT OF 0.5 ms IN DURATION AND 2 nA IN AMPLITUDE ASSUMING A GAIN OF 100 FOR SEVERAL VALUES OF ϵ

ϵ	1	0.9	0.8	0.5	0.1	0.05
α_0	0.000	0.129	0.181	0.357	0.928	1.162
α_1	2.745	2.750	2.756	2.787	3.109	3.446
τ_m (ms)	10.000	10.000	10.000	10.000	10.000	10.000
τ_0 (ms)	10.000	9.856	9.683	8.871	5.373	4.255
τ_S (ms)	10.000	9.000	8.000	5.000	1.000	0.500
τ_1 (ms)	1.171	1.168	1.163	1.140	0.937	0.776
ρ	5.000	4.500	4.000	2.500	0.500	0.25
k	6.565	5.908	5.252	5.282	0.656	0.328
C_0 (V)	0.773	0.767	0.758	0.714	0.385	0.199
C_1 (V)	1.121	1.123	1.124	1.130	1.093	0.900
R_N (MΩ)	100.000	98.182	96.000	85.714	40.000	24.000
E (mV)	80.000	78.545	76.800	68.571	32.00	19.20

Testing of the Shunt Model

Electrical cables of the type described above can be modeled by analog compartmental models of the type shown in Fig. 3. Each compartment represents the lumped impedance of a given region of the membrane surface. R_i represents the axoplasmic or the longitudinal resistance per unit length and R_m and C_m represent the membrane resistance and capacitance per unit length. In Fig. 3, 20 compartments model a neuron with an electrotonic length $L = 1$ and a time constant of 11 ms. The value of $\rho = 4.5$ was chosen to match the average granule cell as reported in Durand et al. (1983). The model was tested with several

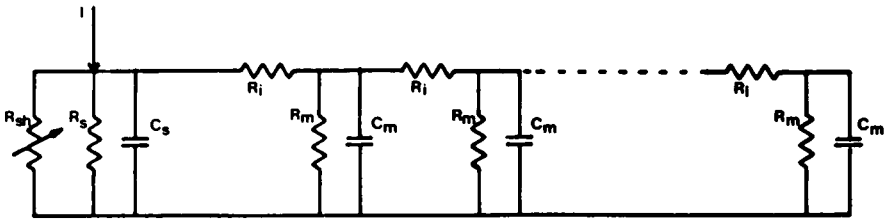

FIGURE 3 Analog compartmental model of an electric cable. 20 compartments, each made up of a resistor R_i for the axoplasmic resistance and R_m, C_m for the membrane parameters model a neuron of electrotonic length: $L = 20\sqrt{R_i/R_m} = 1$. The resistor R_S and C_S model the soma and a shunt resistor R_{SN} is introduced in parallel with R_S for varying ϵ. The resistors were 1% tolerance and the capacitors chosen to give values of $\tau_m = R_mC_m = 11$ ms. $R_i = 825\ \Omega$; $R_m = 332$ kΩ; $R_s = 100$ kΩ; $C_m = 0.033\ \mu$F; $C_S = 0.110\ \mu$F; $L = 1.0$; $R_{NS} = 18.2$ kΩ; $\tau_m = 11$ ms; $\rho_{NS} = 4.5$; ϵ = variable.

shunt resistors, giving several values for ϵ: 1, 0.9, 0.8, 0.5, 0.1, and 0.05. A 0.5-ms, 1.5-mA current pulse was injected at the soma with a constant current generator. The resulting voltage decay was analyzed by a multiexponential decay analysis computer program based on the "peeling" method (Rall, 1969; Durand et al., 1983). The results for C_0, τ_0, C_1, and τ_1 are tabulated in Table II section B. These results are compared in the same table with the theoretical time constants and coefficients calculated from the equations of the model (see Table II section A). A theoretical decay was also calculated from these values, once replaced in Eq. 23, and both the theoretical and experimental voltage decays were plotted in Fig. 4 for $\epsilon = 0.5$. Note the good degree of agreement between the theoretical voltage decay and the voltage decay from the analog model, both in Fig. 4 and Table II, where the relative error is <1.5% for C_0 and τ_1 and <6.6% for C_1 and τ_1. A greater error is expected for the higher-order parameters ($n = 1$) compared with lower-order parameters ($n = 0$) because of the peeling analysis method. It is clear, however, that the modeling equations account for the fast voltage transient caused by a somatic shunt. The inverse problem still remains to be solved. Is it possible to determine the modeling parameters L, ρ, ϵ, and τ_m from the knowledge of C_0, τ_1, C_1, and τ_1?

TABLE II
COEFFICIENTS AND TIME CONSTANTS FOR A CELL WITH $L = 1$, $\rho_{NS} = 4.5$, AND $\tau_m = 11$ ms

	C_0	τ_0	C_1	τ_1
A.				
1	0.965	11.000	1.393	1.317
0.9	0.956	10.820	1.395	1.312
0.8	0.945	10.620	1.398	1.307
0.5	0.885	9.661	1.410	1.279
0.1	0.455	5.727	1.378	1.033
0.05	0.226	4.552	1.123	0.845
B.				
1	0.954	11.050	1.394	1.296
0.9	0.950	10.860	1.450	1.300
0.8	0.936	10.700	1.470	1.289
0.5	0.868	9.800	1.440	1.292
0.1	0.437	5.870	1.362	1.040
0.05	0.227	4.585	1.123	0.811

The theoretical values are tabulated in A for varying values of ϵ while the experimentally measured coefficients and time constants from an analog compartmental model are tabulated in B.

Shunt Model: Solution of Equations

As noted in previous studies (Durand et al., 1983), only C_0, C_1, τ_0, and τ_1 can be measured with good accuracy using multiexponential decay analysis programs. Therefore, from the above derivation, the system of Eqs. 17–20 for $i = 0,1$ and Eq. 21 must be solved. It can easily be shown by substitution that this system of nine equations with nine unknowns, α_0, α_1, β_0, β_1, L, ρ, τ_m, k, and ϵ, can be reduced to a system of two independent equations, using Eq. 20 for $i = 0$ and $i = 1$ with two independent variables, L and τ_m. Once τ_0 and τ_1 are measured, ρ and ϵ can then be calculated as follows:

$$\rho = \frac{\cot(\alpha_0 L)}{\alpha_0 \coth L} \cdot \left[-(1+\alpha_1^2) \cdot \frac{\alpha_1 \tan(\alpha_1 L) - \alpha_0 \tan(\alpha_0 L)}{(1+\alpha_0^2)\alpha_1 \tan(\alpha_1 L) - (1+\alpha_1^2)\alpha_0 \tan(d_0 L)} \right]; \quad (28)$$

$$\epsilon = \frac{\alpha_1 \tan(\alpha_1 L) - \alpha_0 \tan(\alpha_0 L)}{(1+\alpha_0^2)\alpha_1 \tan \alpha_1 L - (1+\alpha_1^2)\alpha_0 \tan \alpha_0 L}. \quad (29)$$

Therefore, it is possible to determine the model parameters from the knowledge of τ_0, C_0, τ_1, and C_1, when the input resistance R_N of the cell and the amplitude of the injected current are known (Eq. 20). A computer program based on an iteration procedure has been designed to solve this system of equations by minimizing the square of the error, SE, between the experimentally measured values of the coefficients EC_0, EC_1, and the theoretical values TC_0 and TC_1: $SE = (C_0 - EC_0)^2 + (TC_1 - EC_1)^2$. However, the input resistance, the gain of the amplifier, and the current are not always accurately known and it is shown below that it is possible to solve the above system of equations based on the knowledge of C_0, τ_0, C_1, and τ_1 alone.

From Eq. 16 we obtain the following relation, since at $T = 0$, $V = 0$: $IR_N = \Sigma_i C_i$. If only the coefficients C_0 and C_1 have been estimated with a reasonable degree of accuracy, we have:

$$IR_N = C_0 + C_1 + RES, \quad (30)$$

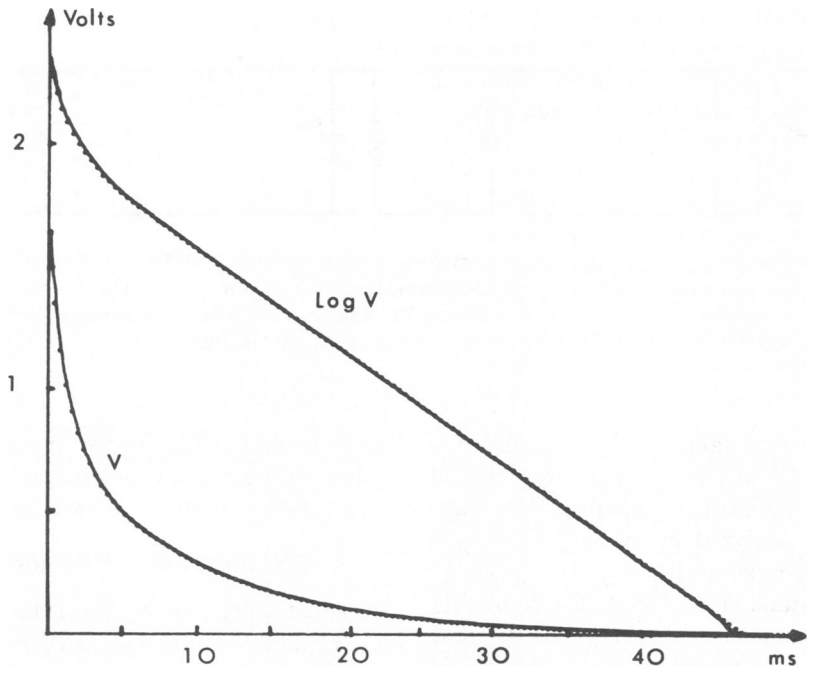

FIGURE 4 Test of the shunt model equations with an analog compartmental model with the following parameters. $L = 1$, $\rho = 2.5$, $\tau_m = 11$ ms, and $\epsilon = 0.5$. The voltage decay following a 0.5-ms, 1.5-mA current pulse injected in the somatic region (solid line, experimental) is fitted to the equation of the voltage decay calculated from the shunt model equations (dotted line, theoretical).

where RES is the residue equal to $C_2 + C_3 + C_4$ (higher-order terms are assumed negligible). If we now define R_i by $C_i = IR_N \cdot R_i$ in Eq. 20, we then have:

$$RES = IR_N \cdot (R_2 + R_3 + R_4), \tag{31}$$

and from Eq. 30 we obtain and equation for the product IR_N:

$$IR_N = \frac{C_0 + C_1}{1 - (R_2 + R_3 + R_4)}, \tag{32}$$

where C_0 and C_1 are known and R_2, R_3, and R_4 can be calculated from $R_i = C_i/IR_N$. These equations then allow the estimation of the model parameters L, ρ, ϵ, and τ_m based only on the measured values of the coefficients and time constant independently of the current injected and the input resistance of the cell.

DISCUSSION

The equations for the voltage decay following the injection of a current pulse in an equivalent cable with a variable shunt at the somatic end and a high-impedance termination at the other were derived. The introduction of this shunt was suggested by the results of experiments in motoneurons and hippocampal cells (Iansek and Redman, 1973; Durand et al., 1983). This shunt model can account for the fast potential decays observed in those neurons, which could not be modeled by the Rall model with a uniform resistance and capacitance specific values (Rall, 1969). The equations provide a method for measuring the shunt at the soma caused by electrode penetration damage or by a lower somatic specific resistance from the knowledge of the time constants and coefficients of the voltage decay. More importantly, however, the introduction of the additional parameter ϵ makes it possible to increase dramatically the proportion of neurons for which a model could be identified. This proportion increased from 40 to 95% in a recent study of the effect of chronic alcoholism on membrane time constant of granule cells (Durand and Carlen, 1984).

Although the model allows the measurement of the magnitude of this somatic shunt, it is not possible to determine whether the shunt is caused by electrode penetration damage or by a low somatic membrane resistance. It may be possible, however, to estimate the relative contribution of these parameters by measuring the shunt during the after-hyperpolarization potential (AHP). This potential can be attributed to a calcium-mediated potassium conductance increase (Hotson and Prince, 1980; Alger and Nicoll, 1980; Gustaffson and Wigstrom, 1981; Thalman and Ayala, 1982) and can be blocked by removing calcium from the extracellular space, injecting EGTA into the cell, or even by blocking the potassium conductance. Therefore, the contribution of the potassium conductance to the somatic shunt could be assessed by measuring ϵ before and after blocking the potassium conductance. Similarly, the contribution of other ions such as chloride could be determined using pharmacological agents.

A somatic shunt, not previously measured with analytical solutions, could explain the variability observed in the estimation of the passive parameters of nerve cells, and particularly the membrane specific resistance and capacitance (Brown et al., 1981; Turner and Schwartzkroin, 1980; Lux and Pollen, 1966; Cole, 1968; Durand et al., 1983). Taking the somatic shunt into account when modeling can give higher specific membrane resistance and lower membrane capacitance values. For example, the coefficients and time constants $C_0 = 0.714$ V, $\tau_0 = 8.87$ ms, $C_1 = 1.13$ V, $\tau_1 = 1.14$ ms calculated for a cell with $L = 1$, $\epsilon = 0.5$, $\rho = 2.5$, $\tau_m = 10$ ms, $S = 500$ μm^2 give, with the constant membrane specific resistance Rall model, $R_m = 1{,}430$ $\Omega.cm^2$ and $C_m = 6.6$ $\mu F/cm^2$. However, taking the shunt as an additional parameter in the modeling, the following results are obtained: $R_{md} = 3{,}000\ \Omega \cdot cm^2$, $R_{ms} = 1{,}500\ \Omega \cdot cm^2$, and $C_m = 3.0\ \mu F/cm^2$. It is clear, in this example, how the introduction of this shunt parameter could explain the higher values for C_m published in the literature.

However, the somatic shunt, although introduced in the model for better fitting of the experimental data, could also be an important functional parameter. As noted in Table I, the localized decrease of the membrane resistance at the soma lowers the time constant of the equalized decay phase τ_0 of the whole neuron, including the dendrites. Therefore, a simple somatic shunt can significantly alter the electrical response of distal dendrites (Carlen and Durand, 1981), and thereby affect and perhaps control dendritic neuronal integration. Decreasing the somatic membrane resistance would lower the time constant, thereby decreasing temporal summation of excitatory postsynaptic potential (EPSP) in the dendrites. Inhibitory potentials, such as the inhibitory postsynaptic potential (IPSP) and the AHP in the hippocampus, also cause increased conductance at the soma, and their function is thought to move the membrane potential away from threshold, but it could also be to alter neuronal integration in the dendrites significantly. Another effect of the somatic shunt is to modify the transfer function of the dendrites. This transfer function of DC potentials in dendrites to soma can be expressed by (Appendix II):

$$T_{DS} = 1/\cosh L \cdot [1 + (\tanh L)^2/\rho_{NS} \cdot \epsilon], \qquad (33)$$

where ρ_{NS} is the dendritic dominance ratio of the cell with no shunt. Fig. 5, based on Eq. 33 shows how the transfer function is affected by increasing shunt amplitudes (smaller ϵ). The transfer of DC potentials from the dendrites to soma is greatly attenuated by increasing the somatic shunt. Therefore, by increasing the membrane conductance at the soma, the cell can not only control the time constant of the membrane in the dendrites but also the amplitudes of potentials reaching the soma. Although many conductance changes at the soma have been measured, their effect on synaptic integration has been little studied and could represent an important neuronal function.

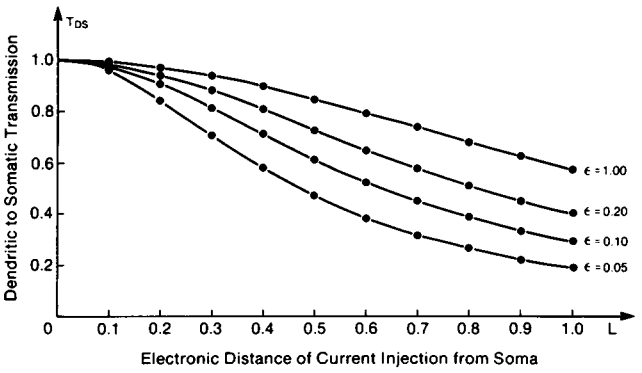

FIGURE 5 Plot of the dendritic to somatic transfer function, T_{DS} of DC potentials vs. the electrotonic distance of current injection for several values of ϵ. Note how the transfer function of potential from distal location is markedly decreased by somatic shunts.

In conclusion, the somatic shunt, introduced to develop a better electrical neuronal model, could have significant functional importance as a neuronal mechanism for controlling neuronal integration. This somatic shunt can be measured using the equations derived for the solution of the cable equation with the modified boundary conditions.

APPENDIX A

Derivation of the Coefficients

From the boundary Eqs. 4 and 10, it can be shown that the coefficients of the modified orthogonality relation (Eq. 15) are: $a_1 = b_1 = 0$ and $b_0 = \epsilon \cdot (\tanh L/\rho)$. Since

$$V(X, \infty) = IR_N \cdot \frac{\cosh (L - X)}{\cosh L}$$

and $X_n = \cos \alpha_n \cdot (L - X)$, we then obtain

$$B_n = \frac{\dfrac{IR_N}{\cosh L}\displaystyle\int_0^L \cosh (L - X) \cdot \cos [\alpha_n(L - X)]\, dX + \dfrac{\epsilon \tanh L}{\rho} \cdot \cosh\alpha_n \cdot IR_N}{\displaystyle\int_0^L \cos^2 [\alpha_n(L - x)]\, dX + \frac{\epsilon \tanh L}{\rho} \cdot \cos^2(\alpha_n L)}. \qquad (A1)$$

By integration, the numerator N of Eq. A1 is equal to:

$$N = \frac{IR_N}{1 + \alpha_n^2} \cdot \cos (\alpha_n L) \cdot \left[\tanh L + \alpha_n \tan (\alpha_n L) + \frac{\epsilon \tanh L}{\rho}(1 + \alpha_n^2)\right]. \qquad (A2)$$

Using Eq. 12, N simplifies to:

$$N = \frac{IR_N}{1 + \alpha_n^2} \cdot \cos (\alpha_n L) \cdot \frac{L}{k}(\rho + 1). \qquad (A3)$$

The integral of the denominator D of Eq. A2 can easily be evaluated

and, therefore:

$$D = \frac{1}{2} \cdot \cos^2(\alpha_n L) \cdot \left(\frac{\tan \alpha_n L}{\alpha_n} + \frac{L}{\cos^2(\alpha_n L)} + \frac{2\epsilon \tanh L}{\rho} \right). \quad \text{(A4)}$$

Using Eq. 12 as above and simple trigonometric equations, D can be expressed by:

$$D = \frac{1}{2} \cdot \cos^2(\alpha_n L) \cdot \frac{L}{k} \cdot \left\{ \frac{1 - \epsilon(1 + \alpha_n^2)}{\alpha_n^2} + 2\epsilon + k + \frac{L^2}{\alpha_n^2 k} \cdot [1 - \epsilon(1 + \alpha_n^2)]^2 \right\}. \quad \text{(A5)}$$

The coefficient B_n is then obtained from $B_n = N/D$:

$$B_n = \frac{1}{\cos(\alpha_n L)} \cdot \frac{IR_N}{1 + \alpha_n^2} \cdot \frac{2(\rho + 1)}{\beta_n + 2\epsilon + k + (\alpha_n L \beta_n)^2/k}; \quad \text{(A6)}$$

where

$$\beta_n = \frac{1 - \epsilon(1 + \alpha_n^2)}{\alpha_n^2}. \quad \text{(A7)}$$

From Eqs. 13 and 14, the voltage at $X = 0$ (recording site) is given by:

$$V(0, T) = IR_N - \sum_n B_n \cos(\alpha_n L) e^{-(1+\alpha_n^2)T}. \quad \text{(A8)}$$

Using Eqs. A6 and A8, the voltage $V(t)$ at $X = 0$ following a step current pulse injected at $X = 0$ is:

$$V(t) = IR_N - \Sigma C_n e^{-t/\tau_n} \quad \text{(A9)}$$

with

$$\tau_n = \tau_m/(1 + \alpha_n^2) \quad \text{(A10)}$$

and

$$C_n = IR_N \cdot \frac{2(\rho + 1)\,\tau_n/\tau_m}{\beta_n + 2\epsilon + k + (\alpha_n L \beta_n)^2/k} \quad \text{(A11)}$$

where α_n solutions of the transcendental Eq. 12 and β_n is given by Eq. A7.

APPENDIX B

Transmission Coefficient

A useful solution of Eq. 1 is:

$$\frac{V}{V_0} = \cosh X + B_1 \sinh X. \quad \text{(B1)}$$

Applying the boundary conditions:

$$X = L \qquad V = V_L$$

$$X = 0 \qquad \left.\frac{\partial V}{\partial X}\right]_{x=0} = \frac{\lambda r_i}{R_s} \cdot V_0,$$

the voltage along the cable can be determined by:

$$V = V_L \cdot \frac{\cosh X + (\lambda r_i/R_s) \sinh X}{\cosh L + (\lambda r_i/R_s) \sinh X}. \quad \text{(B2)}$$

Therefore, the transmission coefficient T_{DS} from dendrite to soma, defined by V_0/V_L, is:

$$T_{DS} = 1/\cosh L \cdot [1 + (\lambda r_i/R_s) \sinh L/\cosh L]. \quad \text{(B3)}$$

Since $\rho = R_s/\lambda r_i \coth L$ and $\rho = \epsilon \rho_{NS}$,

$$T_{DS} = 1/\cosh L[1 + (\tanh L)^2/\epsilon \rho_{NS}]. \quad \text{(B4)}$$

I am grateful to Drs. H. Kunov, W. Rall, and R. Plonsey for discussing the results of the theoretical derivation and reviewing the paper, and to Shirley Light for carefully typing the manuscript.

This work was supported by the Addiction Research Foundation, and National Institutes of Health grant R01-NS-16660-02 to Dr. P. Carlen.

Received for publication 15 September 1983 and in final form 18 April 1984.

REFERENCES

Alger, B. E., and R. A. Nicoll. 1980. Epileptiform burst after hyper polarization: calcium-dependent potassium potential in hippocampal CA1 pyramidal cells. *Science (Wash. DC).* 210:1122–1124.

Brown, T. H., R. A. Fricke, and D. H. Perkel. 1981. Passive electrical constants in three classes of hippocampal neurons. *J. Neurophysiol.* 46:812–827.

Carlen, P. L., and D. Durand. 1981. Modelling the postsynaptic location and magnitude of tonic conductance changes resulting from neurotransmitter or drugs. *Neuroscience.* 6:839–846.

Churchill, R. V. 1942. Expansions in series of non-orthogonal functions. *Am. Math Soc. Bull.* 48:143–149.

Cole, K. S. 1968. Membranes, Ions and Impulses. University of California Press, Berkeley, CA. 12.

Davis, L., and R. Lorente de No. 1947. Contribution to the mathematical theory of electrotonics. *Stud. Rockefeller Inst. Med. Res.* 131:442–496.

Durand, D. 1982. Alcohol induced brain damage—morphology and physiology in the hippocampus. Ph.D. thesis. Biomedical Engineering Institute, University of Toronto, Toronto, Canada.

Durand, D., and P. L. Carlen. 1984. Decreased neuronal inhibition after long-term administration of ethanol in vitro. *Science (Wash. DC).* 224:1349–1361.

Durand, D., and H. Kunov. 1982. Measurement of the electrotonic parameters of small central neurons; the shunt cable model. *Abst. 9th Conf. Can. Med. Biol. Eng. Soc.* 9:79–80.

Durand, D., P. L. Carlen, N. Gurevich, A. Ho, and H. Kunov. 1983. Measurement of the passive electrotonic parameters of granule cells in the rat hippocampus using HRP staining and short current pulses. *J. Neurophysiol.* 50:1080–1096.

Fleshman J. W., I. Seger, S. Culheim, and R. E. Burke. 1983. Matching electrophysiological with morphological measurements in cat α-motoneurons. *Abst. Soc. Neurosci.* 9:341.

Gustaffson, B., and H. Wigstrom. 1981. Evidence for two types of afterhyperpolarization in Ca1 pyramidal cells in the hippocampus. *Brain Res.* 206:462–486.

Hodgkin, A. L., and A. H. Rushton. 1946. The electrical constants of a crustacean nerve fiber. *Proc. R. Soc. Lond. B Biol. Sci.* 133:444–479.

Hotson, J. R., and D. A. Prince. 1980. A calcium-activated hyperpolarization follows repetitive firing in hippocampal neurons. *J. Neurophysiol.* 43:409–419.

Iansek, R., and S. J. Redman. 1973. An analysis of the cable properties of spinal motoneurons using a brief intracellular current pulse. *J. Physiol. (Lond.)*. 234:613–636.

Lux, H. D., and D. A. Pollen. 1966. Electrical constants of neurons in the motor cortex of the cat. *J. Neurophysiol.* 29:207–220.

Rall, W. 1959. Branching density trees and motoneurons membrane resistivity. *Exp. Neurol.* 1:421–527.

Rall, W. 1969. Time constants and electrotonic length constants of membrane cylinders and neurons. *Biophys. J.* 9:1483–1508.

Rall, W. 1977. Core conductor theory and cable properties of neurons. *Handb. Physiol.* 1:39–97.

Thalman, R. H., and G. F. Ayala. 1982. A late increase in potassium conductance following synaptic stimulation of granule neurons of the dentate gyrus. *Neurosci. Lett.* 29:243–248.

Turner, D. A., and P. A. Schwartzkroin. 1980. Steady-state electrotonic analysis of intracellularly stained hippocampal neurons. *J. Neurophysiol.* 44:194–199.